



JULY 15, 2024

To study the association between
unhealthy lifestyle (metabolic
dysfunction) and liver metastasis using
liver microtissue on a dish model.

MAUDI KARIBA SONDER

2599309

BMT PDT AST

Table of Contents

<i>Introduction</i>	2
<i>Materials and Methods</i>	2
Cell Lines.....	2
Spheroid formation	3
Spheroid Growth.....	3
Metabolic Activity	3
Spheroid Staining.....	4
Fluorescent Microscopy	4
Cell Tracking	4
<i>Results</i>	5
Spheroid Size	5
Alamar Blue Assay	6
Immuno- and Lipid Staining.....	7
Structure of the cocultures.....	9
Live Cell Imaging	10
<i>Discussion and Conclusion</i>	11
<i>Recommendations</i>	12

Introduction

Pancreatic cancer accounts for approximately 3% of all new cancer cases every year (1). The overall 5-year survival rate for pancreatic cancer is 13%, rapidly decreasing from 44% for localised cancer, to 16% for regional and 3% for distant pancreatic cancer. Typically, pancreatic cancer is diagnosed at a later stage, when the cancer has already spread, thus decreasing the chances of survival (2). The liver is especially prone to developing a secondary pancreatic tumour, as it has the potential to create a pre-metastatic niche for pancreatic cancer cells (2,3). Hepatic steatosis is especially conducive in forming such a favourable microenvironment for metastasis (4). Hepatic steatosis is one of the beginning stages of MASLD (Metabolic Dysfunction-Associated Steatotic Liver Disease) (5). Leading an unhealthy lifestyle, for example by consuming a high-fat and high-sugar diet, poses a significant risk in developing a form of MASLD.

This paper uses spheroids made from liver tissue to gain a better understanding of the relation between an unhealthy diet and the metastasis of pancreatic cancer in the liver. Spheroids made of hepatocytes (HepaRG) and hepatic stellate cells (LX-2) were cultured in 96-well ultra-low attachment plates. Half of the cultured spheroids were treated with a medium that was high in glucose, fructose and palmitic acid, to model metabolic dysfunction caused by an unhealthy lifestyle with a high-fat and high-sugar diet. The metabolic activity of the spheroids was measured and compared to the control group to confirm the induction of metabolic dysfunction. The spheroids were stained with LipidTox to mark the presence of lipid droplets. Pancreatic cancer cells (Mia-Paca2) labelled with a cell tracker were added to spheroid medium and their extravasation into the spheroid was tracked under a microscope.

Materials and Methods

Cell Lines

The LX-2 cell line is an immortalised human hepatic stellate cell line. These cells were cultured in DMEM-GlutaMAX with 10% FBS and 1% Pen/Strep. HepaRG cells are hepatocyte-like cells derived from a human hepatic progenitor cell line. The HepaRG cells were cultured in William's E. Mia-Paca2 cells are a human pancreatic cancer cell line consisting of epithelial cells. They were cultured in DMEM-GlutaMAX with 10% FBS and 1% Pen/Strep. All cells were cultured in T25 flasks, at 37°C and 5% CO₂. The culture flasks for the HepaRG cells were collagen coated to ensure proper attachment of the cells to the flask. The collagen coating was made by adding 1ml of a 1:100 dilution of 0.5% Collagen (Matrix BioScience) in MilliQ to a flask and incubating at 37°C for at least an hour. To passage the cells, the cell monolayer was washed twice with ~2mL PBS and treated for 5 minutes at 37°C with 500µL Trypsin/EDTA or Tryple, for LX-2 and HepaRG cells respectively.

Spheroid formation

The spheroids were cultured on 96-well ultra-low attachment plates at 5000 cells per well. LX-2s and HepaRGs were seeded in mono- and cocultures. The LX-2 and HepaRG cocultures were seeded at a 1:10 ratio. Live cell concentration of the two cell lines was measured using a Luna-II automatic cell counter, by adding 10 μ L of a 1:1 ratio of cells with Trypan blue to a counting slide. This live cell concentration was used to make mono- and coculture cell suspensions of the desired concentration (~25,000 cells per mL) in William's Medium E with GlutaMAX, 10% FBS, 1% Pen/Strep, glutamine, hydrocortisone and insulin. To prevent evaporation from affecting spheroid formation, the edges of the plate were filled with PBS. All other wells were filled with 200 μ L of cell suspension. After seeding the spheroids, the plate was spun down for 1 minute at 2000 rotations p/m to promote the aggregation of the cells. Spheroid medium was changed every two to three days. To prevent the loss of spheroids when changing the medium, only half (100 μ L) of the medium was removed and replaced with new medium. From day 3 onward, half the spheroids were given a GFIP medium consisting of the William's E control medium with high concentrations of fructose (5 mM), glucose (25 mM) and palmitic acid (240 μ M) to mimic metabolic dysfunction (6). When adding the GFIP medium for the first time these concentrations were doubled, since only half of the old medium is changed every time. In another plate of spheroids, one third of spheroids was given the control William's Medium E, another third of spheroids received the same GFIP medium as described above and the last third of spheroids received a GFI medium, which is identical to the GFIP medium without the addition of palmitic acid.

Spheroid Growth

Spheroids were imaged daily (not including weekends) with the Nikon TI-E inverted microscope using the Hokawo imaging software. Images were taken with the 4x objective connected to a Hamamatsu Orca Flash 4.0 v2 CCD camera. ImageJ was used to analyse the change in size of the spheroids over time.

Metabolic Activity

An Alamar Blue assay was performed to compare the metabolic activity of the control group to the GFIP and GFI treated spheroids. For this assay, 25 μ L of Alamar Blue reagent (Invitrogen) was added to each well containing a spheroid, while keeping exposure to light to a minimum. The spheroids with added Alamar Blue reagent were then incubated in the dark at 37°C and 5% CO₂. After 24 hours, 150 μ L of medium was removed from each well and transferred to a black bottom 96-well plate. The assay readout was done using a VICTOR™ X3 Multimode Plate Reader, the results were normalized to the spheroids receiving the control medium.

Spheroid Staining

To prepare the spheroids for staining, 100 μ L of culture medium was removed from each well and replaced with 100 μ L of fixation solution. This fixation solution consists of a 1:10 dilution of 37% paraformaldehyde in filtered PBS. This was incubated for 30 minutes at room temperature. After removing the fixative, spheroids were washed twice with PBS. The spheroids were then stained with primary and secondary antibodies for type I collagen, DAPI for the nuclei and LipidTox for lipid droplets. All incubation steps for the fixation, immuno- and lipid staining were done at room temperature, using 100 μ L of staining solution per well. Each washing step uses 200 μ L of either PBS or 1%BSA/PBS per well. Starting off with the primary antibody, Goat Anti – Type I Collagen (0.4 mg/mL, Southern Biotech) diluted 1:100 in PBS was added to each well and incubated for 90 minutes. After removing the primary antibodies, spheroids were washed 3 times with 1%BSA/PBS. A 1:100 dilution of Alexa Fluor 488 Donkey Anti-Goat (2mg/mL, Invitrogen) in 1%BSA/PBS was added as a secondary fluorescent antibody and incubated for 60 minutes in the dark. The antibodies were removed after incubation and spheroids were washed 3 times with 1%BSA/PBS. DAPI diluted 1:100 in PBS was added as a nuclei stain and incubated for 30 minutes in the dark. After removing the staining solution, the spheroids were washed with PBS twice. The final staining solution was a 1:1000 dilution of HCS LipidTox™ Deep Red Neutral Lipid stain (Invitrogen) in 1%BSA/PBS. This was incubated in the dark for 30 minutes. After removing the staining solution and washing with PBS twice, the spheroids were kept in MilliQ, if imaged directly, or in Aquatex mounting. After staining the plate was stored in the dark at 4°C

Fluorescent Microscopy

Images of the stained spheroids were made using the Nikon TI-E inverted microscope as well as the Zeiss LSM880 confocal microscope. To obtain a higher resolution image, some spheroids were moved to a 15 well glass bottom μ slide (Ibidi). Spheroids were moved from a round bottom plate to a microscopy slide using a 1000 μ L pipet tip with the end cut off, to ensure the spheroid was not damaged while moving it. Images made on the Nikon TI-E inverted microscope were edited with ImageJ, and the images from the confocal microscope were edited in Zeiss Zen Lite.

Cell Tracking

A fluorescent cell tracker was added to the Mia-Paca2 cells to follow their extravasation into the spheroids. The cells were labelled by resuspending them in 2ml of medium with a 5 μ M concentration of Cell Tracker Green CMFDA (Invitrogen) and incubating for 30 minutes at 37°C. After incubation the cells were centrifuged to remove the cell tracker working solution and resuspended in 2%FBS/PBS. This cell suspension containing Mia-Paca2 cells with Cell Tracker Green (CTG) was added to wells with live LX-2 and HepaRG coculture spheroids, at ~100,000 cells per well. Imaging of the cell invasion was done live on the Nikon TI-E inverted microscope. The

Zeiss LSM880 confocal microscope was used to image spheroids that were fixed 24, 72 and 96 hours after adding the Mia-Paca2 cells with CTG.

To determine the distribution of LX-2 and HepaRG cells within a spheroid, the method to add a fluorescent tracker to cells as described above was used to label LX-2 cells with CTG and HepaRG cells with Cell Tracker Blue CMAC (Invitrogen). The labelled cells were then resuspended in William's E control medium at a 1:10 ratio and seeded at 5000 cells per well in a 96-well ultra-low attachment plate. These spheroids were fixed after 5 days and imaged using the Zeiss LSM880 confocal microscope.

Results

Spheroid Size

All spheroids were kept in the control medium until day 3. After pictures of the spheroids were taken on day 3, the medium of all spheroids was changed, and half the spheroids received GFIP medium instead of control medium. There is no data on spheroid size for day 5 and 6, since these days fell in a weekend. The LX-2 monocultures formed larger and rounder spheroids than the HepaRG monocultures (figure 1). HepaRG monocultures that were given the GFIP medium lost their round shape and appear to disintegrate over time. The coculture spheroids are comparable in size to the HepaRG spheroids but are shaped more like the LX-2 spheroids. The average size of the different spheroids (determined using ImageJ) over time is represented in figure 2. On average the LX-2 monocultures are larger than both the HepaRG monocultures and the coculture spheroids. The HepaRG spheroids increase in size between day 4 and day 7. The HepaRG and LX-2 coculture spheroids are relatively steady in size over the course of 8 days. There is no notable difference in spheroid size between the control group and the GFIP treated coculture spheroids.

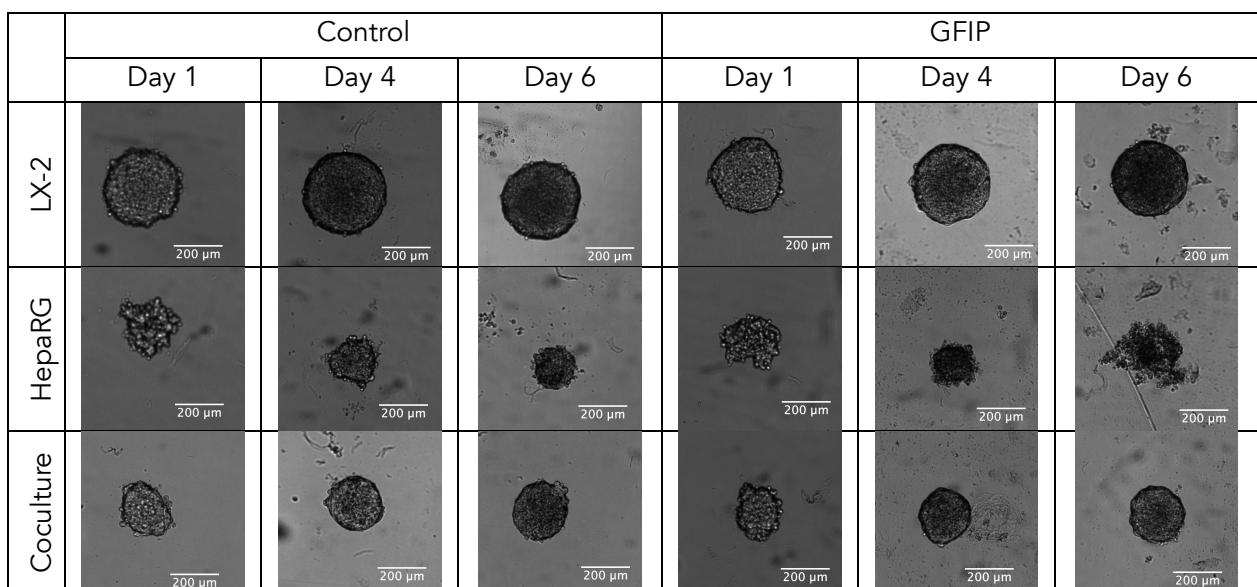


Figure 1: Pictures of the different spheroids taken on day 1, 4 and 8 after seeding. All spheroids were seeded in control medium, GFIP medium was added from day 3 onward.

Average Spheroid Size

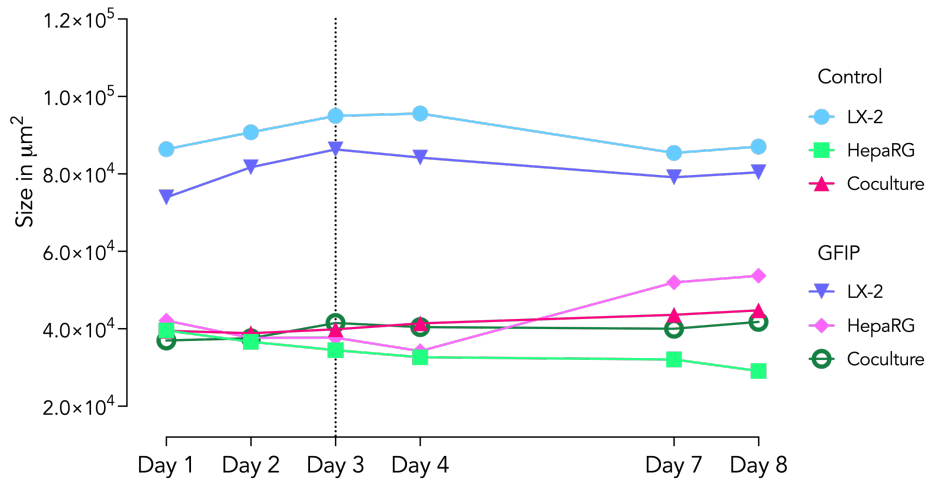


Figure 2: Representation of the average size of LX-2 and HepaRG mono- and coculture spheroids. The GFIP medium was added for the first time on day 3, after the images to assess spheroid size were made.

Alamar Blue Assay

The results from the first Alamar Blue Assay are represented in figure 3. The Alamar Blue reagent was added to the wells 24 hours after changing the medium. Spheroids that were given a GFIP medium showed a higher metabolic activity than the control spheroids.

The Alamar Blue Assay was repeated on a different plate of spheroids where one third of the spheroids was given the control medium, another third was kept in GFI medium, and the rest was given GFIP medium. The Alamar Blue reagent was added to the wells 48 hours after changing the medium. The results of the assay are represented in figure 4. There is no difference metabolic activity between control medium and GFI medium. Like the first Alamar Blue Assay, spheroids given the GFIP medium show a higher metabolic activity than those kept in control medium. The average metabolic

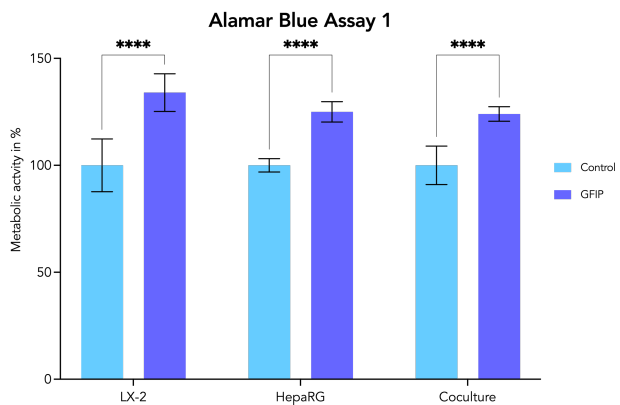


Figure 1: First Alamar Blue assay results. Average metabolic activity of each type of control spheroid is represented as 100% and compared to the average metabolic activity of the respective GFIP treated spheroid.

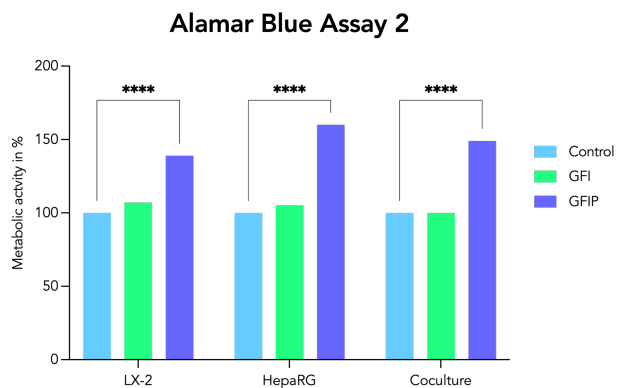


Figure 2: Second Alamar Blue assay results. Average metabolic activity of each type of control spheroid is represented as 100% and compared to the average metabolic activity of the respective GFI and GFIP treated spheroids.

activity of all GFIP spheroids in this second assay is higher than in the first assay. An outlier in the results for the LX-2 monocultures in GFIP, indicating a metabolic activity of 237%, caused a large standard deviation and a much higher average of the results. The outlier was replaced with the average of the values without the outlier resulting in a metabolic activity more in line with expectations, based on the first assay.

Immuno- and Lipid Staining

All but one of the stained spheroids were lost after the first attempt of staining the spheroids (figure 5). The remaining spheroid was an LX-2 monoculture grown in control medium. The images were taken with the 4x objective of the inverted microscope.

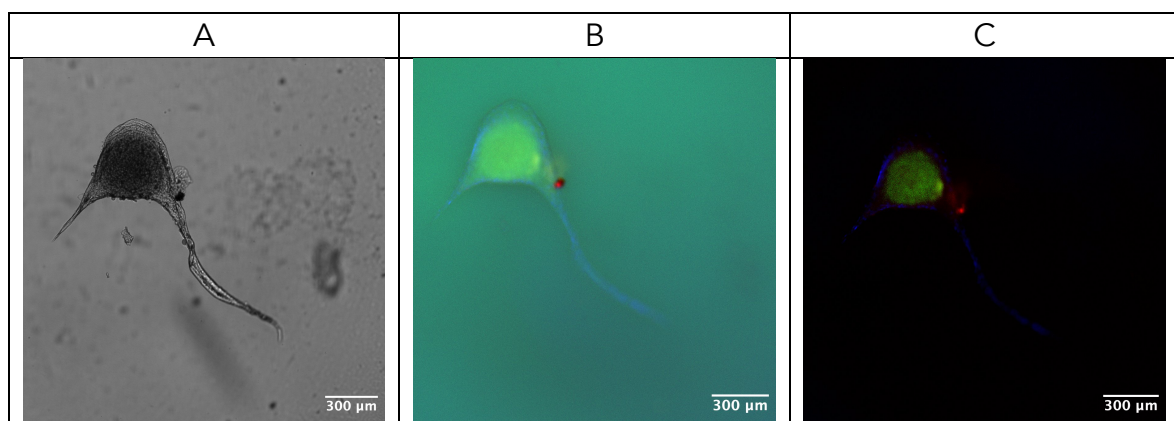


Figure 3: LX-2 monoculture spheroid remaining after first attempt of spheroid staining. A: image of the spheroid made using brightfield. B: Composite image of the FITC, DAPI and APC channels of the Nikon T-IE inverted microscope. C: Composite of the same channels as B, manually adjusted for background noise.

During the first staining, spheroids were kept in about 50 μ L of fluid in between each step. Because so many spheroids were lost during the first try, the staining protocol was repeated leaving about 100 μ L of fluid in the wells at all times. The stained spheroids were mounted in Aqua Tex. Figure 6 shows images of a control coculture taken with the Nikon TI-E inverted microscope. The top row of images are the unedited pictures from the FITC, DAPI and APC channel of the microscope and the result of merging these three channels. To remove the background noise, the minimum and maximum brightness and contrast levels were adjusted in ImageJ to obtain a black background. These images were then also merged. The unedited composite pictures of the fluorescent images look very similar for all spheroids (figure 7). Adjusting the contrast and brightness to remove the colour from the background does result in a clearer outline of the spheroid but also causes a loss of intensity of fluorescent signal on the spheroid itself.

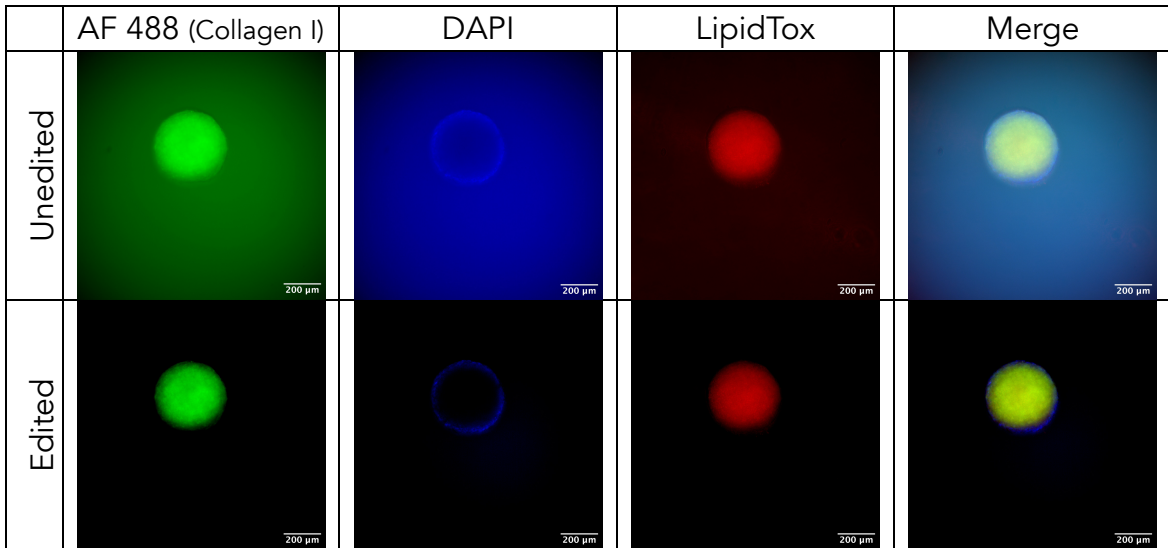


Figure 4: Fluorescent images of a control coculture spheroid made on the Nikon TI-E microscope. The images on the bottom row were adjusted in ImageJ to remove the background noise.

The Zeiss LSM880 confocal microscope was also used to image the stained spheroids. The first spheroid that was imaged using the confocal microscope can be seen in figure 8. Like the images made on the inverted microscope, the image from the confocal microscope contains a lot of background noise. This could be caused by unbound staining that remains in the wells, despite washing the spheroids with PBS. The thick plastic and round bottom of the well plate may also interfere with the

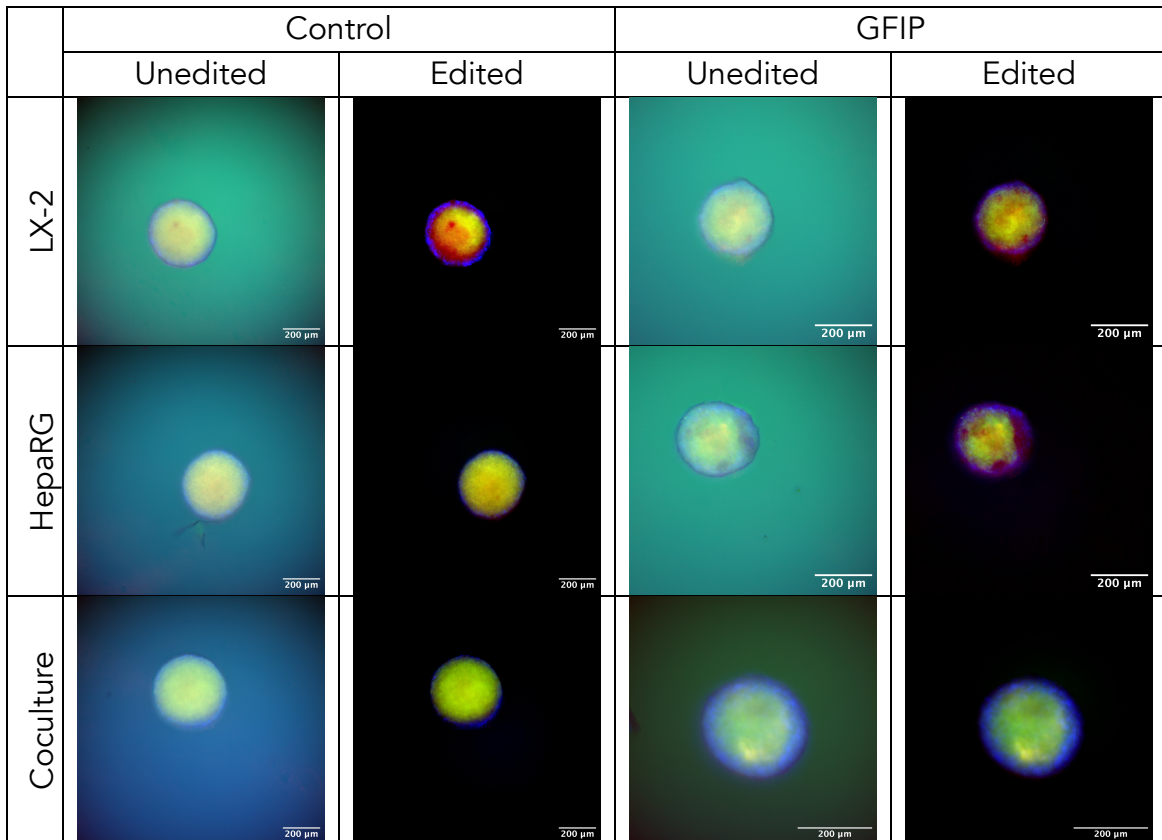


Figure 5: Unedited and edited fluorescent images of the different spheroids in control and GFIP medium.

resolution and overall imaging qualities of the microscope. This might also be why spheroids appear to be shaped like a curved platelet, similar to the shape of a red blood cell.

A new set of spheroids was stained to make sure that the fluorescent signals from the staining had not yet been washed out. For better imaging results, some spheroids were moved to a glass bottom microscopy slide with microwell inserts. A coculture spheroid imaged on a glass bottom μ well slide using the confocal microscope can be seen in figure 9. The DAPI staining on this spheroid is the most distinct, clearly staining the individual nuclei on the outside of the spheroid. Overall, the image is much less noisy than the image in figure 8. There is no speckle in the background from the DAPI staining, and only a little from the AF 488 (Collagen I) and the LipidTox. The spheroids imaged on glass were shaped more like a dome.

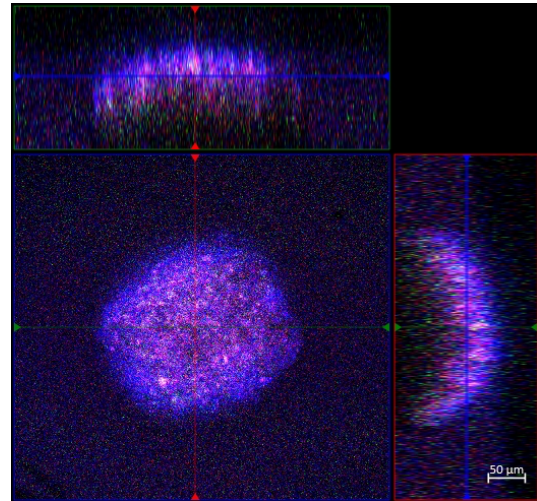


Figure 6: The orthographic projections of the Z-stack of a stained coculture spheroid, imaged on Zeiss LSM880 confocal microscope.

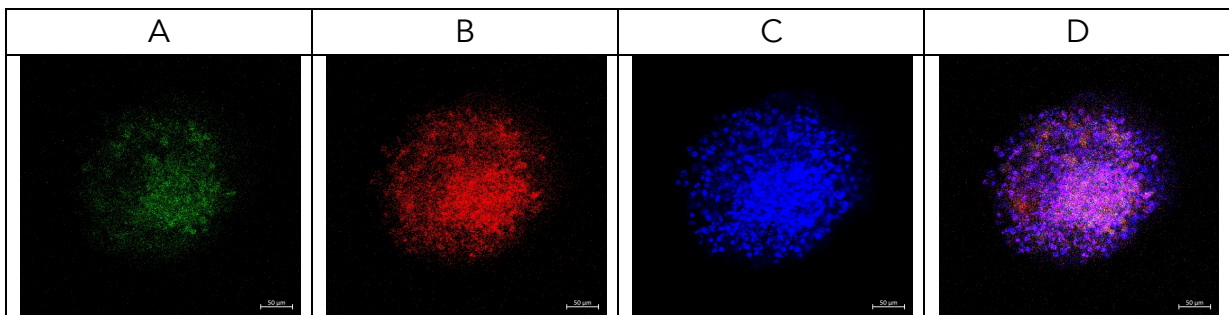


Figure 9: Coculture spheroid on a glass bottom microscope slide imaged with a confocal microscope. A: Signal from AF 488 staining, B: Signal from LipidTox staining, C: Signal from DAPI staining, D: Composite of all fluorescent staining signals.

Structure of the cocultures

It was not possible to determine the distribution of the HepaRG and LX-2 cells within the spheroid by using information from the staining. Spheroids made with HepaRG cells labelled with CTB and LX-2 cells labelled with CTG were imaged with the confocal microscope to gain a better understanding of the structure of the spheroid. From figure 10 we gather that LX-2 cells reside mainly around the edges of the spheroid while the HepaRG cells are found mostly in the centre of the spheroid.

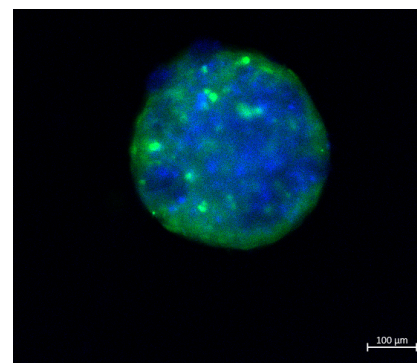


Figure 10: Coculture with LX-2 cells labeled with CTG and HepaRG cells labeled with CTB.

Live Cell Imaging

Mia-Paca2 cells labelled with CTG were added to control and GFIP treated spheroids. These spheroids were laid under the inverted microscope to look at the movement of the Mia-Paca2 cells (figure 11). Because the inverted microscope cannot image inside the spheroid it is impossible to know if the cancer cells are passing over/under the spheroid or entering the spheroid and starting a secondary tumour. To see if any cancer cells entered the spheroids, more labeled Mia-Paca2 cells were added to control and GFIP treated spheroids. One third of these spheroids was fixed 24hrs after adding the cancer cells, another third was fixed after 72hrs, and the last spheroids were fixed after 96hrs (figure 12). There is no notable difference in invasion of cancer cells between the spheroids fixed after 24 and 72 hours. In both cases some Mia-Paca2 cells (green) have gathered around the edges of the spheroid. At 96 hours after adding the cancer cells to the spheroid medium, some of the labeled cells appear to be inside the spheroid.

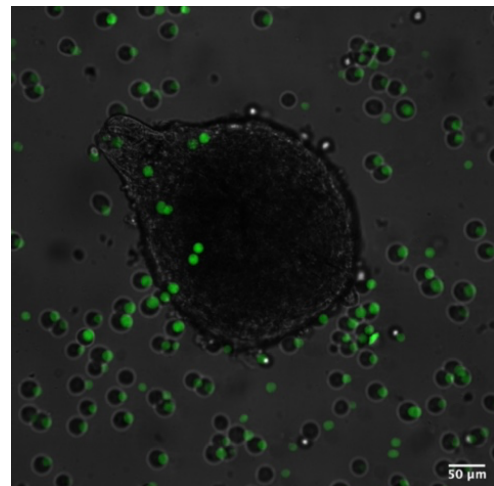


Figure 7: Brightfield image of a spheroid merged with FITC image of the CTG labeled Mia-Paca2 cells.

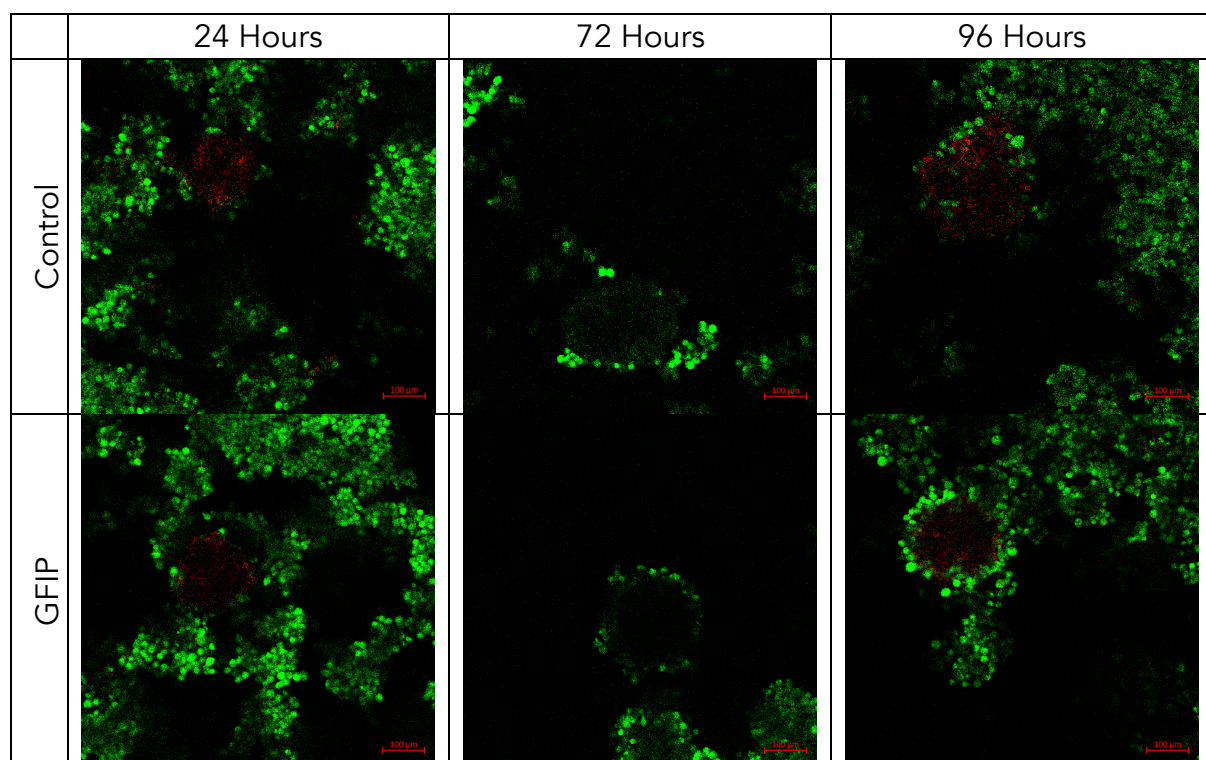


Figure 8: CTG labeled Mia-Paca2 cells were added to spheroid medium and fixated after 24, 72 and 96 hours.

Discussion and Conclusion

From the average size of the spheroids over time, it appears that the LX-s spheroids that were given a GFIP medium are smaller than the control LX-2 spheroids. However, all spheroids were kept in control medium until day 3 and the difference in size was noticeable from the first day onward. The difference in size between the control and GFIP LX-2 spheroids was therefore not caused by the different medium. The HepaRG monocultures considerably increase in size after adding the GFIP medium. This increase in size might be due to the apparent disintegration of these spheroids after adding the GFIP medium. It should be noted that the precise concentration of insulin in both media is unknown. The aim was to add 1nM of insulin to the William's E medium, however the concentration of the stock from which the insulin was added turned out to be different than what we thought it was when adding it to the medium.

The Alamar Blue Assay shows a significant increase in metabolic activity for the spheroids that were given the GFIP medium. Spheroids that were given a GFI medium do not have a higher metabolic activity than the control spheroids. Thus, the addition of palmitic acid is crucial in quickly inducing metabolic dysfunction in liver spheroids.

Staining the spheroids proved to be more difficult than expected. Spheroid staining protocols generally call for permeabilization of the spheroids using Triton X (7,8) However, in this paper the spheroids were not permeabilized before staining because that could have caused the lipid droplets to be removed, which would influence the outcome of the LipidTox staining. Because the spheroids were not permeabilized, the immunostaining (for Collagen I) and the Lipidtox were likely unable to reach the parts of the spheroids that would have bound these stains. Due to the incomplete staining no conclusion can be made regarding a difference in lipid droplet presence in the GFIP spheroids. Spheroids were stained with Collagen I partly to determine the distribution of HepaRG and LX-2 cells within the cocultures, since LX-2 spheroids generally have a higher expression of Collagen I (8). Since this staining, too, did not work, these results cannot be used to draw any conclusions on the distribution of cells in the spheroids. The overall imaging results were better when using the confocal microscope to image spheroids that were placed on a glass slide, however, from the Z-stacks that were made the spheroids appear to be more dome shaped than round. This might be because of the sub-optimal staining, which makes it harder to properly image the spheroid, but the spheroid might also lose its shape when it is moved out of the low attachment well.

From the spheroids made with the cell tracker labelled LX-2 and HepaRG, we conclude that the LX-2 cells reside mainly around the edges of the spheroid, while the most HepaRGs are found in the middle of the spheroid. This is in line with the distribution of these cell types in liver tissue, where hepatic stellate cells are found

mostly between hepatocytes and the sinusoidal endothelial cells, in what is called the space of Disse (9).

It is possible to image live cells with both the inverted and confocal microscope, however, we were unable to capture the live invasion of the spheroid by labelled Mia-Paca2 cells. The inverted microscope can be used to make a video or time lapse of the spheroid and the added cancer, but this video does not give much information on the extravasation of de Mia-Paca2 cells into the spheroid. The Hokowa software used to make the video cannot use the fluorescent function of the microscope, thus making it hard to distinguish between the spheroid and the cancer cells around the edges of, or right below the spheroid. Furthermore, there is no way to tell if a cell that appears to disappear into the spheroid truly did enter the spheroid or is simply passing over the top of it. It is possible to overlay the image with the fluorescent trackers of the Mia-Paca2 cells with a brightfield image of the spheroid, but this still gives limited information on the extravasation of the cells into the spheroid.

Ideally the trajectory of the cancer cells would have been tracked with the confocal microscope, by making a Z-stack of a spheroid multiple times over the course of a few hours. However, because of limited availability of the confocal microscope this was not an option. Alternatively, the confocal microscope was used to image spheroids that were fixed 24, 72 and 96 hours after the labelled cancer cells were added. Because confocal microscope is specifically made for fluorescent imaging, the spheroids in these images are a little hard to distinguish. The spheroids fixed after 24 and 72 hours do not appear to have been invaded by any of the Mia-Paca2 cells, but there are some cancer cells in the spheroids that were fixed 96 hours after adding the cells to the medium. It could be that the extravasation of the cancer cells into the spheroid takes several days, another explanation might be that, by that time, the Mia-Paca2 cells depleted the medium around the spheroid, consequently weakening the spheroid and making it easier to invade.

Recommendations

The staining protocol that was used in this paper was not optimised for spheroids. In hindsight, incubating the spheroids overnight with LipidTox and DAPI might have produced better staining results without needing to permeabilize the spheroids. In another article (10) spheroids made of primary human hepatocytes were successfully stained with Hoechst and NileRed by incubating them overnight, making this a likely solution to the lipid staining issue. Incubating the immunostaining for collagen I overnight probably would not make much of a difference, because the antibodies are too large to enter the cells unless they have been permeabilized. Another option to obtain better staining results without having to permeabilize the cells would be to cryosection the spheroids into thin slices.

If the confocal microscope is used to track the extravasation of cancer cells into the spheroid, the spheroid too should be stained with a fluorescent dye suitable for live cell imaging. Optional dyes would be DAPI or a fluorescent membrane dye. The most important considerations when choosing a dye are that it is non-toxic and of a different excitation wavelength than the cell tracker added to the cancer cells. Spheroids must be thoroughly washed after staining to prevent any left-over staining from adhering to the cancer cells after they are added to the medium. To image the spheroids, it is advised to move them onto a glass bottom slide with as little fluid as possible, to obtain the best imaging results.

References

1. SEER, National Cancer Institute. NIH. 2024 [cited 2024 Jul 13]. Cancer Stat Facts: Pancreatic Cancer. Available from: <https://seer.cancer.gov/statfacts/html/pancreas.html>
2. Liu Z, Gou A, Wu X. Liver metastasis of pancreatic cancer: the new choice at the crossroads. *Hepatobiliary Surg Nutr*. 2023 Feb;12(1):88–91.
3. Shi H, Li J, Fu D. Process of hepatic metastasis from pancreatic cancer: biology with clinical significance. *J Cancer Res Clin Oncol*. 2016;142(6):1137–61.
4. Kim SJ, Hyun J. Altered lipid metabolism as a predisposing factor for liver metastasis in MASLD. *Mol Cells*. 2024;47(2).
5. Chan WK, Chuah KH, Rajaram RB, Lim LL, Ratnasingam J, Vethakkan SR. Metabolic Dysfunction-Associated Steatotic Liver Disease (MASLD): A State-of-the-Art Review. *J Obes Metab Syndr*. 2023 Sep 30;32(3):197–213.
6. Prins GH, Luangmonkong T, Oosterhuis D, Mutsaers HAM, Dekker FJ, Olinga P. A Pathophysiological Model of Non-Alcoholic Fatty Liver Disease Using Precision-Cut Liver Slices. *Nutrients*. 2019 Feb 27;11(3):507.
7. Bergdorf KN, Phifer CJ, Bechard ME, Lee MA, McDonald OG, Lee E, et al. Immunofluorescent staining of cancer spheroids and fine-needle aspiration-derived organoids. 2021 Jun.
8. Cuvellier M, Ezan F, Oliveira H, Rose S, Fricain JC, Langouët S, et al. 3D culture of HepaRG cells in GelMa and its application to bioprinting of a multicellular hepatic model. *Biomaterials*. 2021;269.
9. Kamm DR, McCommis KS. Hepatic stellate cells in physiology and pathology. *J Physiol*. 2022 Apr 30;600(8):1825–37.
10. Kozyra M, Johansson I, Nordling Å, Ullah S, Lauschke VM, Ingelman-Sundberg M. Human hepatic 3D spheroids as a model for steatosis and insulin resistance. *Sci Rep*. 2018 Sep 24;8(1).